



HAL
open science

Backstepping leaderless dynamic consensus among nonlinear systems over directed networks: application to attitude synchronisation control

Maitreyee Dutta, Antonio Loria, Elena Panteley, Sukumar Srikant

► To cite this version:

Maitreyee Dutta, Antonio Loria, Elena Panteley, Sukumar Srikant. Backstepping leaderless dynamic consensus among nonlinear systems over directed networks: application to attitude synchronisation control. 22nd World Congress of the International Federation of Automatic Control (IFAC 2023), Jul 2023, Yokohama, Japan. IFAC-PapersOnLine, vol. 56, no. 2, pp. 1192-1197. hal-03869850

HAL Id: hal-03869850

<https://hal.science/hal-03869850>

Submitted on 16 Jan 2023

HAL is a multi-disciplinary open access archive for the deposit and dissemination of scientific research documents, whether they are published or not. The documents may come from teaching and research institutions in France or abroad, or from public or private research centers.

L'archive ouverte pluridisciplinaire **HAL**, est destinée au dépôt et à la diffusion de documents scientifiques de niveau recherche, publiés ou non, émanant des établissements d'enseignement et de recherche français ou étrangers, des laboratoires publics ou privés.



Distributed under a Creative Commons Attribution 4.0 International License

Backstepping leaderless dynamic consensus among nonlinear systems over directed networks: application to attitude synchronisation control [★]

Maitreyee Dutta ^{*} Antonio Loria ^{**,*★} Elena Panteley ^{**,*★}
Srikant Sukumar ^{*}

^{*} *Systems and Control Engineering Department, IIT Bombay, India*

^{**} *Laboratoire des signaux et systèmes, CNRS, 3, Rue Joliot Curie, 91192, Gif-sur-Yvette, France*

Abstract: We present a distributed consensus controller for multi-agent homogeneous nonlinear systems over directed networks. The systems are assumed to be of second order and the control design relies on a standard backstepping approach. In that light, the control design also hinges on the ability to construct a strict Lyapunov function for the multi-agent nonlinear system interconnected over a directed graph for which the only assumption is that it is connected. That is, that there exists a directed spanning tree, but there is no requirement of conservative conditions such as strong or balanced connectivity. To construct a strict Lyapunov function, we use a generalised Lyapunov equation for the directed-graph Laplacian matrix, which characterises the spanning-tree-existence condition. Then, we establish exponential stability of the consensus manifold. In addition, we implement our dynamic consensus controller on a multi-agent satellite system in the context of attitude synchronisation and demonstrate its efficacy in numerical simulations.

Keywords: Leaderless consensus, backstepping, Lyapunov stability theory, multi-agent systems

1. INTRODUCTION

Collation and synergisation among dynamical systems participating in an complex interconnected network can be broadly categorised as either leader-follower or leaderless consensus. As the name suggests, in leader-follower consensus, the response of the assigned singular leader dictates the desired response of the follower agents. If a directed network is a spanning tree, a singular node that has no incoming edge can directly or indirectly interact with all other nodes in the network; this is the leader of the network. In other cases, a virtual leader is assigned a priori which can act as a yardstick for the remaining systems. On the other hand, leaderless consensus is useful for applications where the nature of the *consensus equilibrium* is not as important as the interacting agents behaving synonymously (Ren, 2009). Leaderless consensus is advantageous in applications exhibiting swarm behaviour, such as opinions coagulation in social networks, symbiotic relationship in biological systems, search and rescue, scientific reconnaissance, security, rendezvous or even attitude synchronisation of unmanned aerial vehicles, to name a few. By opting for leaderless configuration, the collected behaviour is not influenced by a single member and each agent can act independently to any adverse circumstance (Rao and Ghose, 2013). In a directed network, this concept translates into confluence of behaviour of all the agents

that can transmit information to all the other agents in the communication topology to form the collective consensus behaviour.

Backstepping control has been proved to be efficacious in establishing leader-follower consensus over not only undirected-graph but also directed-graph networks in concatenation with different distributed control methods, such as finite-time consensus control (Tian et al., 2018; Shahvali et al., 2018), adaptive fuzzy control (Zhao et al., 2019; Du et al., 2022), neuro adaptive control (Shahvali et al., 2020), event triggered adaptive neural network based sliding mode control (Chen et al., 2021), command filtered approach (Cui et al., 2016), non-smooth backstepping control (Du et al., 2012) to name a few. The so-called leader present in the leader-follower consensus scheme in the context of directed graphs generally implies a virtual leader or a single root node.

Some of the available works that highlight leaderless consensus among the participating systems which rendezvous through unilateral connections include event-triggered approach for general linear (Chen et al., 2022; Wu et al., 2022) or nonlinear systems (Rehan et al., 2021; Ahmed et al., 2021; Long et al., 2022), distributed adaptive approach for general linear systems (Mei et al., 2014; Lv et al., 2017), (Li and Ding, 2015) or Lipschitz nonlinear dynamics (Liu et al., 2016), finite time control among double integrators (He and Wang, 2017) or second order nonlinear systems (Wang et al., 2017), matrix decomposition among linear systems (Zhou et al., 2015).

^{*} This work was supported by the CEFIPRA under the grant number 6001-A

^{**}E. Panteley and A. Loria's work is also supported by the ANR (project HANDY, contract number ANR-18-CE40-0010).

Distributed adaptive output consensus among systems with strict feedback structure is covered in (Huang et al., 2020). Some additional works that cover special cases include leaderless consensus among discrete time systems with first and second-order dynamics, as explored in (Kim et al., 2014), consensus among fractional order single and double integrator is proposed in (Bai et al., 2018). However, several of these works rely on communication topology being strongly connected or balanced, which eases the control design and analysis at the price of certain conservatism—*cf.* (Rehan et al., 2021; Ahmed et al., 2021; Long et al., 2022; Mei et al., 2014; Lv et al., 2017; Li and Ding, 2015; Liu et al., 2016). If the Lyapunov functions used for stability analysis is non-strict then this brings about the requirement of additional tools such as La Salle’s invariance principle and Barb alat’s Lemma—*cf.* (Chen et al., 2022; Wu et al., 2022). Moreover, some of the procedures like finite time distributed consensus rely on non-smooth control—*cf.* (He and Wang, 2017; Wang et al., 2017; Bai et al., 2018).

Some strides made regarding leaderless consensus among agents colluding through directed network using the principles of backstepping control are detailed in (Miao and Chen, 2016; Wang and Gao, 2014). In (Wang and Gao, 2014), each agent is assigned an individual reference system and it is ensured that the reference systems can reach concurrence among themselves using feedback which is dependent on global information, namely, the minimum eigenvalue of the Laplacian matrix. In (Miao and Chen, 2016), the leaderless consensus problem is converted into stabilization problem of edge based state by using edge Laplacian agreement. Here, the control input design is non-smooth even in absence of any parameter uncertainties or disturbances.

In this manuscript, we propose a smooth distributed backstepping-based controller for leaderless state consensus among second-order nonlinear systems interacting over directed connected networks. It is assumed that each agent has nonlinear dynamics transformable into a strict feedback form. We establish global exponential stability of the synchronisation manifold and we provide a constructive proof, *i.e.*, we provide a strict Lyapunov function.

Then, we apply our proposed control method to solve a problem of attitude synchronisation among rigid bodies. Attitude synchronisation refers to application of feedback control input which ensures that a multitude of 3-D rigid bodies have same orientation eventually (Sarlette et al., 2009). Attitude synchronisation is indispensable in formation of satellites. For instance, in the European space agency sponsored infrared space interferometry based Darwin mission, whose objective is to detect exo-planets and capture images of these astrophysical objects with unprecedented spatial resolution (Fridlund, 2004), on-orbit self assembly and satellite swarms for coordinated observations (Izzo and Pettazzi, 2005).

The remainder of the paper is organised as follows: in Section 2 we give a detailed problem formulation and recall some technical statements, fundamental to our analysis, our the main result is presented in Section 3 and in Section 4 we propose a formation controller for rigid bodies. The paper is wrapped up with some concluding remarks in Section 5.

2. SYSTEM DESCRIPTION AND PROBLEM FORMULATION

We consider N identical nonlinear agents with strict feedback structure which is given by

$$\dot{x}_{1i} = f_1(x_{1i}) + g(x_{1i})x_{2i}, \quad (1a)$$

$$\dot{x}_{2i} = f_2(x_{1i}, x_{2i}) + u_i, \quad \forall i = \{1, \dots, N\}, \quad (1b)$$

where $x_{ji} \in \mathbb{R}^n$ for $j = \{1, 2\}$, $u_i \in \mathbb{R}^n$, $f_1 : \mathbb{R}^n \rightarrow \mathbb{R}^n$, $f_2 : \mathbb{R}^n \times \mathbb{R}^n \rightarrow \mathbb{R}^n$ are locally Lipschitz and smooth functions, and $g : \mathbb{R}^n \rightarrow \mathbb{R}^{n \times n}$ is a positive or negative definite matrix such that $g(\cdot) \neq 0$. The control objective is to ensure that

$$\lim_{t \rightarrow \infty} \|x_{1i}(t) - x_{1j}(t)\| \rightarrow 0, \quad (2a)$$

$$\lim_{t \rightarrow \infty} \|x_{2i}(t) - x_{2j}(t)\| \rightarrow 0 \quad \forall j \neq i \quad (2b)$$

under the standing assumption that the digraph $\mathcal{G} = (\mathcal{V}, \mathcal{E})$ is connected, *i.e.*, that it contains a directed spanning tree. The strength of a particular unilateral link \mathcal{E}_{ij} is captured by element $a_{ij} \geq 0$ whereby $a_{ij} > 0$ if j^{th} agent can transmit information to the i^{th} agent else $a_{ij} = 0$. The static communication graph can be portrayed concisely by means of the Laplacian matrix $\mathcal{L} \in \mathbb{R}^{N \times N}$ whose elements are $l_{ii} = \sum_{j \in \mathcal{N}_i} a_{ij}$ and $l_{ij} = -a_{ij} \forall i \neq j$.

For further development, we recall two important statements that hold for connected graphs. The first is a well-known statement on the properties of the Laplacian matrix and the second provides a basis to construct strict Lyapunov functions for multi-agent systems interconnected over generic directed graphs.

Lemma 1. Ren and Beard (2005, 2008) If a directed network has a directed spanning tree, then the Laplacian matrix $\mathcal{L} = [l_{ij}] \in \mathbb{R}^{N \times N}$ has a singular zero eigenvalue and $N - 1$ eigenvalues have strictly positive real part. That is,

$$\sigma_1(\mathcal{L}) = 0, \quad \Re\{\sigma_k(\mathcal{L})\} > 0, \quad k = \{2, \dots, N\}.$$

On the other hand, the right eigenvector of the zero eigenvalue is $\mathbf{1}_N = [1 \ 1 \ \dots \ 1]^\top$ and the left eigenvector v_l satisfies $\sum_{k=1}^N v_{l_k} = 1$ and $v_l^\top \mathcal{L} = 0_N^\top$.

Lemma 2. (Panteley et al., 2020) Let us consider a directed graph \mathcal{G} of order N containing a spanning tree and its Laplacian matrix is $\mathcal{L} \in \mathbb{R}^{N \times N}$. Then, for any positive definite symmetric matrix $Q_L \in \mathbb{R}^{N \times N}$ and $\alpha \in \mathbb{R}^+$, there exists another positive definite symmetric matrix $P_L \in \mathbb{R}^{N \times N}$ such that

$$P_L \mathcal{L} + \mathcal{L}^\top P_L = Q_L - \alpha [P_L \mathbf{1}_N v_l^\top + v_l \mathbf{1}_N^\top P_L]. \quad (3)$$

Now, to analyse the collective behaviour of the multi-agent system we start by rewriting its dynamics in the compact form,

$$\dot{x}_1 = F_1(x_1) + G(x_1)x_2, \quad (4a)$$

$$\dot{x}_2 = F_2(x_1, x_2) + u, \quad (4b)$$

where $x_j = [x_{j1}^\top \ \dots \ x_{jN}^\top]^\top$ for $j = \{1, 2\}$,

$$F_1(x_1) = [f_1(x_{11})^\top \ \dots \ f_1(x_{1N})^\top]^\top,$$

$$F_2(x_1, x_2) = [f_2(x_{11}, x_{21})^\top \ \dots \ f_2(x_{1N}, x_{2N})^\top]^\top$$

$$G(x_1) = \begin{bmatrix} g(x_{11}) & 0_{n \times n} & \dots \\ 0_{n \times n} & g(x_{12}) & \dots \\ \vdots & \vdots & \\ 0_{n \times n} & \dots & g(x_{1N}) \end{bmatrix}.$$

Then, the collective behaviour of (4) is assessed by two dynamical systems evolving in orthogonal spaces (Panteley and Loría, 2017). The first corresponds to a mean-field dynamics with a state defined, roughly speaking, as a weighted average defined by the left eigen-vector corresponding to the unique null eigenvalue of the Laplacian. The second corresponds to the difference between the individual systems' states and the mean-field state; this defines a synchronisation error. That is, we define

$$x_{1m} = (v_l^\top \otimes I_n)x_1, \quad e_1 = [(I_N - \mathbf{1}_N v_l^\top) \otimes I_n]x_1, \\ x_{2m} = (v_l^\top \otimes I_n)x_2, \quad e_2 = [(I_N - \mathbf{1}_N v_l^\top) \otimes I_n]x_2,$$

where $x_{1m}, x_{2m} \in \mathbb{R}^n$, are the mean-field states and $e_1, e_2 \in \mathbb{R}^{Nn}$, are the synchronisation errors. Then, we say that the systems are (resp. achieve) in dynamic consensus if $e_i = 0$ (resp. $e_i \rightarrow 0$). Indeed, on the synchronisation manifold

$$\mathcal{M} = \{e \in \mathbb{R}^{2Nn} : e = 0\}, \quad (5)$$

the individual systems behave according to the mean-field dynamics, given by

$$\dot{x}_{1m} = (v_l^\top \otimes I_n)[F_1(x_1) + G(x_1)x_2], \\ \dot{x}_{2m} = (v_l^\top \otimes I_n)[F_2(x_1, x_2) + u].$$

In turn, the dynamics of the synchronisation errors are given by

$$\dot{e}_1 = \Pi F_1(x_1) + \Pi G(x_1)x_2, \quad (6a)$$

$$\dot{e}_2 = \Pi F_2(x_1, x_2) + \Pi u, \quad (6b)$$

where we introduced the projection matrix

$$\Pi := (I_N - \mathbf{1}_N v_l^\top) \otimes I_n \quad (7)$$

for further development.

Thus the synchronisation control design consists in determining a control law u that stabilises the origin for (6). To that end, we design a backstepping distributed controller.

3. BACKSTEPPING CONTROL DESIGN

Under the standing assumption that the digraph is connected, let Lemma 2 generate a symmetric positive-definite matrix P_L such that (3) holds. Then, consider the function $V_1 : \mathbb{R}^{Nn} \rightarrow \mathbb{R}_{\geq 0}$, defined as $V_1(e_1) = e_1^\top (P_L \otimes I_n)e_1$ and which is positive-definite and decrescent. Moreover, its total derivative along the trajectories of (6a) yields

$$\dot{V}_1(e_1) = 2e_1^\top (P_L \otimes I_n)\Pi F_1(x_1) + 2e_1^\top (P_L \otimes I_n)e_2^w, \quad (8)$$

where $e_2^w := \Pi G(x_1)x_2$ is regarded as a virtual control input. Indeed, if $e_2^w = e_{2d}^w := -\Pi F_1(x_1) - e_1$,

$$\dot{V}_1(e_1) = -2e_1^\top (P_L \otimes I_n)e_1. \quad (9)$$

Next, we introduce $\tilde{e} := e_2^w - e_{2d}^w$, which satisfies

$$\tilde{e} = \Pi[G(x_1)x_2 + F_1(x_1) + x_1] \quad (10)$$

and, therefore,

$$\dot{\tilde{e}} = \Pi \left[\overbrace{G(x_1)}^{\cdot} x_2 + G(x_1)[F_2(x_1, x_2) + u] + \left[\frac{\partial F_1(x_1)}{\partial x_1} + I_{Nn} \right] [F_1(x_1) + G(x_1)x_2] \right]. \quad (11)$$

Then, consider the control Lyapunov function candidate

$$V_2(e_1, \tilde{e}) = e_1^\top (P_L \otimes I_n)e_1 + \gamma \tilde{e}^\top (P_L \otimes I_n)\tilde{e}, \quad \gamma > 0,$$

which is positive definite and decrescent for all $(e_1, \tilde{e}) \in \mathbb{R}^{Nn} \times \mathbb{R}^{Nn}$. Its total derivative along the trajectories of (6a)-(11) yields

$$\dot{V}_2(e_1, \tilde{e}) = 2e_1^\top (P_L \otimes I_n)(\tilde{e} - e_1) + 2\gamma \tilde{e}^\top (P_L \otimes I_n) \times \\ \Pi \left[\overbrace{G(x_1)}^{\cdot} x_2 + G(x_1)[F_2(x_1, x_2) + u] + \left[\frac{\partial F_1(x_1)}{\partial x_1} + I_{Nn} \right] [F_1(x_1) + G(x_1)x_2] \right].$$

We see that, defining

$$u = -F_2(x_1, x_2) + G(x_1)^{-1} \left[-\overbrace{G(x_1)}^{\cdot} x_2 - [\mathcal{L} \otimes I_n]\tilde{e} - \left[\frac{\partial F_1(x_1)}{\partial x_1} + I_{Nn} \right] [F_1(x_1) + G(x_1)x_2] \right], \quad (12)$$

we obtain

$$\dot{V}_2(e_1, \tilde{e}) = -2e_1^\top [P_L \otimes I_n]e_1 + 2e_1^\top [P_L \otimes I_n]\tilde{e} - \gamma \tilde{e}^\top ([P_L \mathcal{L} + \mathcal{L}^\top P_L] \otimes I_n)\tilde{e}. \quad (13)$$

Now, after Lemma 2, the last term on the right-hand side of the previous expression equals to

$$\tilde{e}^\top ([Q_L - \alpha(P_L \mathbf{1}_N v_l^\top + v_l \mathbf{1}_N^\top P_L)] \otimes I_n)\tilde{e}$$

for any $\alpha > 0$ and $Q_L = Q_L^\top > 0$. However, upon expanding the term $((P_L \mathbf{1}_N v_l^\top) \otimes I_n)\tilde{e}$, using (7), (10), $v_l^\top \mathbf{1}_N = 1$, and the properties of the Kronecker product, we obtain

$$[(P_L \mathbf{1}_N v_l^\top (I_N - \mathbf{1}_N v_l^\top)) \otimes I_n][G(x_1)x_2 + F_1(x_1) + x_1] \\ = [P_L(\mathbf{1}_N v_l^\top - \mathbf{1}_N v_l^\top) \otimes I_n][G(x_1)x_2 + F_1(x_1) + x_1] = 0.$$

We conclude that

$$\dot{V}_2(e_1, \tilde{e}) = -2e_1^\top [P_L \otimes I_n]e_1 + 2e_1^\top [P_L \otimes I_n]\tilde{e} - \gamma \tilde{e}^\top [Q_L \otimes I_n]\tilde{e}. \quad (14)$$

Using the triangle inequality, we obtain

$$\dot{V}_2(e_1, \tilde{e}) \leq -[2p_{L_m} - \frac{1}{\varepsilon}]|e_1|^2 - [\gamma q_{L_m} - \varepsilon p_{L_M}^2]|\tilde{e}|^2, \quad (15)$$

where $\varepsilon > 0$ and k_m and k_M denote lower and upper-bounds for $z^\top Kz$, for a square matrix K . It is clear that \dot{V}_2 is negative definite for appropriate values of ε and γ , for any given Q_L and P_L . Thus, from the previous developments we draw the following statement.

Proposition 3. Consider the multi-agent system (4) in closed loop with (12), (10), and (7), under the standing assumption that the underlying graph is directed and connected. Then, the synchronisation manifold \mathcal{M} in (5) is globally exponentially stable. Therefore, the multi-agent system (1) achieves dynamic consensus, that is,

$$\lim_{t \rightarrow \infty} \|x_{1i}(t) - x_{1m}(t)\| \rightarrow 0, \quad \lim_{t \rightarrow \infty} \|x_{2i}(t) - x_{2m}(t)\| \rightarrow 0, \\ \text{so (2) hold.}$$

Proof. For the system (6a)-(11) in closed loop with (12), (15) holds. The right-hand side of this inequality is negative definite if, for any given Q_L and corresponding P_L ,

$$\varepsilon > \frac{1}{2p_{L_m}}, \quad \gamma > \frac{\varepsilon p_{L_M}^2}{q_{L_m}}. \quad (16)$$

Since V_2 is positive definite and radially unbounded, it follows that $\{(e_1, \tilde{e}) = (0, 0)\}$ is globally exponentially stable. On the other hand, note that $e_1 = 0$ implies that $x_1 = (\mathbf{1}_N \otimes x_{1m})$, so, from (10) and using $e_1 = \Pi x_1$,

it follows that $(e_1, \tilde{e}) = (0, 0)$ implies that $\Pi[G(x_1)x_2 + F_1(x_1)] = 0$. On the other hand,

$$\begin{aligned} \Pi F_1(x_1) &= \Pi \begin{bmatrix} f_1(x_{11}) \\ \vdots \\ f_1(x_{1N}) \end{bmatrix} = \Pi \begin{bmatrix} f_1(x_{1m}) \\ \vdots \\ f_1(x_{1m}) \end{bmatrix} \\ &= [(I_N - \mathbf{1}_N v_l^\top) \otimes I_n] [\mathbf{1}_N \otimes f_1(x_{1m})] \\ &= 0_{Nn}, \end{aligned}$$

so $\Pi[G(x_1)x_2 + F_1(x_1)] = 0$ is equivalent to $\Pi G(x_1)x_2 = 0$. In turn, the latter is equivalent to

$$\begin{aligned} \Pi G(x_1)x_2 &= \Pi \begin{bmatrix} g(x_{11}) & 0_{n \times n} & \cdots \\ \vdots & \vdots & \vdots \\ \cdots & 0_{n \times n} & g(x_{1N}) \end{bmatrix} x_2 \\ &= \Pi \begin{bmatrix} g(x_{1m}) & 0_{n \times n} & \cdots \\ \vdots & \vdots & \vdots \\ \cdots & 0_{n \times n} & g(x_{1m}) \end{bmatrix} x_2 \\ &= \Pi(I_N \otimes g(x_{1m}))x_2 = [(I_N - \mathbf{1}_N v_l^\top) \otimes g(x_{1m})]x_2 = 0 \\ &\iff [I_N \otimes g(x_{1m})]e_2 = 0 \\ &\iff e_2 = 0. \end{aligned}$$

The last equation holds true as $g(\cdot)$ is either a positive or negative definite matrix as per the given assumption. The statement follows. \blacksquare

4. ATTITUDE SYNCHRONISATION OF RIGID BODIES

We consider now a multi-agent network in which each node consists of a rigid body—*cf.* Tsiotras (1996); Shuster et al. (1993). We are primarily concerned with synchronising the attitude (orientation) of such a network of spacecraft modelled as rigid bodies. This is critical in several space applications such as Earth observation (EO) (Folta et al., 2002; Neeck et al., 2005), terrestrial planet finder (TPF) (Lawson, 2001), space telescope assembly (STA), stellar imager (SI) and synthetic aperture imaging (SAI) (Kang and Sparks, 2002). This is primarily motivated by reduced size of each spacecraft and increased robustness in a multi-spacecraft formation. Euler's parameters are typically used to describe the rigid body rotation about an inertial (Earth Centered Inertial) axis. The frame rotating with the rigid body is called the 'body-fixed frame'. The Euler's parameters can be uniquely reduced to any set of three parameters by using a suitable transformation. The Rodrigues parameters are one such commonly used set with the transformation from Euler's parameters briefly recounted below as per the details given in Schaub et al. (1996).

Let Θ be the principal rotation angle and \hat{n} be the normal unit vector. Then, the Euler's parameters are

$$\sigma_0 = \cos\left(\frac{\Theta}{2}\right), \quad \sigma_k = \hat{n}_k \sin\left(\frac{\Theta}{2}\right), \quad k \in \{1, 2, 3\} \quad (17)$$

$$\sigma^\top \sigma = \sigma_0^2 + \sigma_1^2 + \sigma_2^2 + \sigma_3^2 = 1, \quad (18)$$

where $\sigma = [\sigma_0 \ \sigma_1 \ \sigma_2 \ \sigma_3]^\top$. The Euler's parameters σ_k have to conform to the holonomic constraint as given in (18) which quite naturally describes a three dimensional unit sphere in \mathbb{R}^4 . The transformation from the Euler's parameters to the Rodrigues parameters are defined as

$$\rho_k = \frac{\sigma_k}{\sigma_0}, \quad k = 1, 2, 3. \quad (19)$$

It is important to note that the Rodrigues parameters encounter a singularity at $\sigma_0 = 0$ which corresponds to a principal rotation angle, $\Theta = \pm 180$. In the multi-agent setting considered for simulations with five rigid bodies in a network, the kinematics equations in terms of the Rodrigues parameters $\rho_i = [\rho_{1i} \ \rho_{2i} \ \rho_{3i}]^\top$, $i \in \{1, \dots, 5\}$, which represents the attitude of the i -th rigid body, are given by

$$\dot{\rho}_i = (I_3 + \rho_i^\times + \rho_i \rho_i^\top) \omega_i, \quad (20)$$

where $\omega_i \in \mathbb{R}^3$ is angular velocity of the i -th rigid body in a body-fixed frame. Then, the Euler's equations of rotational motion are

$$J \dot{\omega}_i = -(\omega_i^\times J \omega_i) + u_i, \quad i = \{1, \dots, 5\}, \quad (21)$$

where $J \in \mathbb{R}^{3 \times 3}$, such that $J = J^\top > 0$, represents the moment of inertia for the rigid body, $u_i \in \mathbb{R}^3$ is the input torque, and for a vector $a \in \mathbb{R}^3$, a^\times represents the vector cross product. The input torque u is usually produced by external actuators such as gas jets in the spacecraft context.

In compact form, (20)-(21) can be written as

$$\dot{\rho} = \text{blkdiag} \{R(\rho_i)\} \omega = R(\rho) \omega \quad (22a)$$

$$(I_5 \otimes J) \dot{\omega} = -\text{blkdiag} \text{col}(\omega_i^\times J \omega_i) + u \quad (22b)$$

where $R(\rho_i) = I_3 + \rho_i^\times + \rho_i \rho_i^\top$, $\rho = [\rho_1 \ \rho_2 \ \rho_3 \ \rho_4 \ \rho_5]^\top$, $\omega = [\omega_1 \ \omega_2 \ \omega_3 \ \omega_4 \ \omega_5]^\top$, $u = [u_1 \ u_2 \ u_3 \ u_4 \ u_5]^\top$. Indeed the control objective in this setup is to ensure $\lim_{t \rightarrow \infty} \|\rho_i(t) - \rho_{im}(t)\| = 0$ and subsequently $\lim_{t \rightarrow \infty} \|\omega_i(t) - \omega_{im}(t)\| = 0 \ \forall \ i = \{1, \dots, 5\}$ such that $\rho_{im}(t), \omega_{im}(t)$ are the corresponding mean field values given by $\rho_{im} = (v_l^\top \otimes I_3) \rho$ and $\omega_{im} = (v_l^\top \otimes I_3) \omega$. Comparing (20)-(21) to (1) yields

$$\begin{aligned} x_{1i} &:= \rho_i, \quad x_{2i} := \omega_i, \quad f_1(x_{1i}) := 0_3, \quad g(x_{1i}) := R(\rho_i), \\ f_2(x_1, x_2) &:= -\omega_i^\times J \omega_i. \end{aligned} \quad (23)$$

Then, based on derived feedback control input (12), the control torque that needs to be applied to each of the agent is given by

$$\begin{aligned} u_i &= (\omega_i^\times J \omega_i) + J R(\rho_i)^{-1} \left[-\dot{R}(\rho_i) \omega_i - R(\rho_i) \omega_i \right. \\ &\quad \left. - \sum_{j \in \mathcal{N}_i} a_{ij} ((R(\rho_i) \omega_i + \rho_i) - (R(\rho_j) \omega_j + \rho_j)) \right]. \end{aligned} \quad (24)$$

The interaction graph between the agents is represented by the graph in Figure 1.

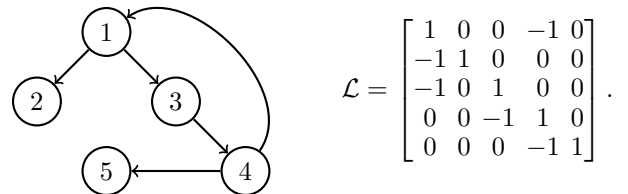


Fig. 1. Connected digraph and its corresponding Laplacian

Arbitrary and distinct initial conditions are assigned to the five agents. As per the given graph, the first, third, and fourth agents can transmit information to all the

other nodes in the graph. Indeed, the eigenvector v_l in this specific case is given by $\begin{bmatrix} \frac{1}{3} & 0 & \frac{1}{3} & \frac{1}{3} & 0 \end{bmatrix}^\top$.

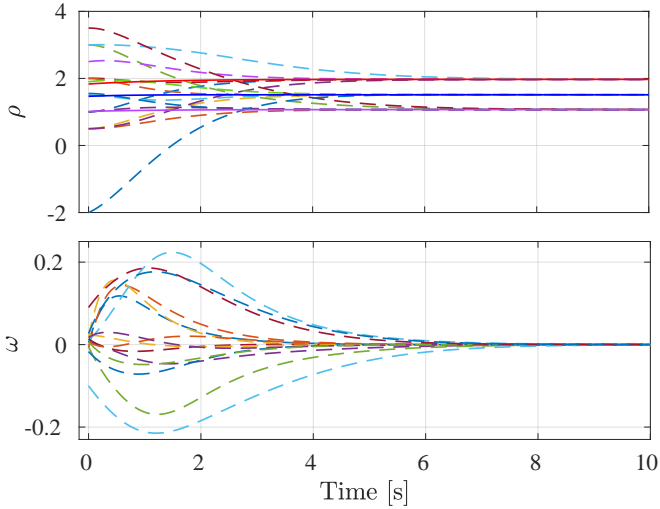


Fig. 2. Consensus among five agents with rigid body dynamics.

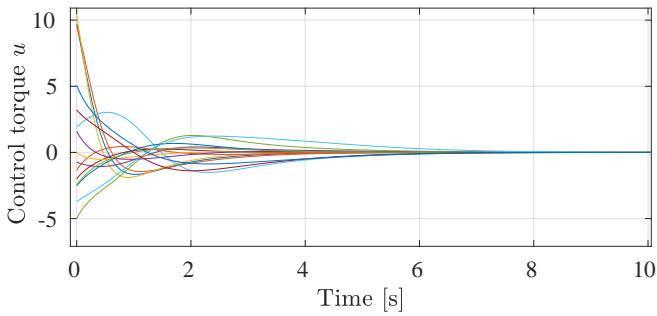


Fig. 3. Control torque applied to the interconnected rigid bodies.

The simulation result can be seen in Figures 2 and 3 above. It can be seen that the $\rho_i, \omega_i, \forall i \in \{1, \dots, 5\}$ for each of the agents reaches the mean-field value which is given by $\rho_m = \frac{1}{3}(\rho_1 + \rho_3 + \rho_4)$ and $\omega_m = \frac{1}{3}(\omega_1 + \omega_3 + \omega_4)$ respectively. In the first subplot of Figure 2, the bold red, purple and navy blue plots represents the mean-field values specifically for $\rho_{1i}, \rho_{2i}, \rho_{3i} \forall i \in \{1, \dots, 5\}$ respectively. In the second subplot of Figure 2, the angular velocity ω converges to zero as the attitude of individual rigid bodies synchronises with the other agents. Figure 3 displays the behaviour of the control torque applied to the interconnected system which complements the conclusion drawn from Figure 2.

5. CONCLUSION

We proposed a Lyapunov-based distributed controller for leaderless consensus of second-order nonlinear systems. The control design relies on the classical backstepping method. The difficulty involved in multi-agent systems is the construction of a strict Lyapunov function. Yet, our results apply to generic connected directed graphs. The efficacy of the method was demonstrated by designing an attitude synchronisation controller for multi-agent rigid-bodies. For simplicity, in this paper the controller relies on

a feedback-linearizing inner control loop, but we believe that the procedure may be used to design less stringent controllers, such as passivity-based. Also, the fact that a strict Lyapunov function is explicitly computed, sets the basis for further research on robust consensus control with respect to external disturbances, measurement noise, sensor attacks, etc. These topics are subject of future research.

REFERENCES

- Ahmed, I., Rehan, M., and Iqbal, N. (2021). A novel exponential approach for dynamic event-triggered leaderless consensus of nonlinear multi-agent systems over directed graphs. *IEEE Transactions on Circuits and Systems II: Express Briefs*, 69(3), 1782–1786.
- Bai, J., Wen, G., and Rahmani, A. (2018). Leaderless consensus for the fractional-order nonlinear multi-agent systems under directed interaction topology. *International Journal of Systems Science*, 49(5), 954–963.
- Chen, C., Lewis, F.L., and Li, X. (2022). Event-triggered coordination of multi-agent systems via a lyapunov-based approach for leaderless consensus. *Automatica*, 136, 109936.
- Chen, T., Yuan, J., and Yang, H. (2021). Event-triggered adaptive neural network backstepping sliding mode control of fractional-order multi-agent systems with input delay. *Journal of Vibration and Control*, 10775463211036827.
- Cui, G., Xu, S., L. Lewis, F., Zhang, B., and Ma, Q. (2016). Distributed consensus tracking for non-linear multi-agent systems with input saturation: a command filtered backstepping approach. *IET Control Theory & Applications*, 10(5), 509–516.
- Du, H., Li, S., and Shi, P. (2012). Robust consensus algorithm for second-order multi-agent systems with external disturbances. *International Journal of Control*, 85(12), 1913–1928.
- Du, Z., Liang, H., and Ahn, C.K. (2022). Adaptive fuzzy control for multi-agent systems with unknown measurement sensitivity via a simplified backstepping approach. *IEEE Transactions on Circuits and Systems II: Express Briefs*.
- Folta, D., Bristow, J., Hawkins, A., and Dell, G. (2002). Nasa’s autonomous formation flying technology demonstration, earth observing-1 (eo-1). In *International Symposium: Formation Flying Missions and Technology*.
- Fridlund, C. (2004). The darwin mission. *Advances in Space Research*, 34(3), 613–617.
- He, X. and Wang, Q. (2017). Distributed finite-time leaderless consensus control for double-integrator multi-agent systems with external disturbances. *Applied Mathematics and Computation*, 295, 65–76.
- Huang, J., Wang, W., Wen, C., Zhou, J., and Li, G. (2020). Distributed adaptive leader–follower and leaderless consensus control of a class of strict-feedback nonlinear systems: A unified approach. *Automatica*, 118, 109021.
- Izzo, D. and Pettazzi, L. (2005). Equilibrium shaping: distributed motion planning for satellite swarm. In *Proc. 8th Intern. Symp. on Artificial Intelligence, Robotics and Automation in space*, volume 25.
- Kang, W. and Sparks, A. (2002). Coordinated attitude and formation control of multi-satellite systems. In

- AIAA Guidance, Navigation, and Control Conference and Exhibit*, 4655.
- Kim, J.M., Park, J.B., and Choi, Y.H. (2014). Leaderless and leader-following consensus for heterogeneous multi-agent systems with random link failures. *IET Control Theory & Applications*, 8(1), 51–60.
- Lawson, P.R. (2001). The terrestrial planet finder. In *2001 IEEE Aerospace Conference Proceedings (Cat. No. 01TH8542)*, volume 4, 4–2005. IEEE.
- Li, Z. and Ding, Z. (2015). Distributed adaptive consensus and output tracking of unknown linear systems on directed graphs. *Automatica*, 55, 12–18.
- Liu, W., Zhou, S., Qi, Y., and Wu, X. (2016). Leaderless consensus of multi-agent systems with lipschitz nonlinear dynamics and switching topologies. *Neurocomputing*, 173, 1322–1329.
- Long, J., Wang, W., Huang, J., Lü, J., and Liu, K. (2022). Adaptive leaderless consensus for uncertain high-order nonlinear multiagent systems with event-triggered communication. *IEEE Transactions on Systems, Man, and Cybernetics: Systems*.
- Lv, Y., Li, Z., Duan, Z., and Feng, G. (2017). Novel distributed robust adaptive consensus protocols for linear multi-agent systems with directed graphs and external disturbances. *International Journal of Control*, 90(2), 137–147.
- Mei, J., Ren, W., Chen, J., and Anderson, B.D. (2014). Consensus of linear multi-agent systems with fully distributed control gains under a general directed graph. In *53rd IEEE Conference on Decision and Control*, 2993–2998. IEEE.
- Miao, Z.M. and Chen, W. (2016). Backstepping-based high-order nonlinear consensus for multi agent system via edge laplacian. In *2016 IEEE Chinese Guidance, Navigation and Control Conference (CGNCC)*, 1045–1050. IEEE.
- Neeck, S.P., Magner, T.J., and Paules, G.E. (2005). Nasa’s small satellite missions for earth observation. *Acta Astronautica*, 56(1-2), 187–192.
- Panteley, E. and Loria, A. (2017). Synchronization and dynamic consensus of heterogeneous networked systems. *IEEE Trans. on Automatic Control*, 62(8), 3758–3773. doi:10.1109/TAC.2017.2649382.
- Panteley, E., Loria, A., and Sukumar, S. (2020). Strict lyapunov functions for consensus under directed connected graphs. In *Proc. European Control Conference (ECC)*, 935–940. St. Petersburg, Russia. doi: 10.23919/ECC51009.2020.9143719.
- Rao, S. and Ghose, D. (2013). Sliding mode control-based autopilots for leaderless consensus of unmanned aerial vehicles. *IEEE transactions on control systems technology*, 22(5), 1964–1972.
- Rehan, M., Tufail, M., and Ahmed, S. (2021). Leaderless consensus control of nonlinear multi-agent systems under directed topologies subject to input saturation using adaptive event-triggered mechanism. *Journal of the Franklin Institute*, 358(12), 6217–6239.
- Ren, W. and Beard, R.W. (2005). Consensus seeking in multiagent systems under dynamically changing interaction topologies. *IEEE Transactions on automatic control*, 50(5), 655–661.
- Ren, W. and Beard, R.W. (2008). *Distributed consensus in multivehicle cooperative control*, volume 27 of 2. Springer verlag, London: Springer London.
- Ren, W. (2009). Distributed leaderless consensus algorithms for networked euler–lagrange systems. *International Journal of Control*, 82(11), 2137–2149.
- Sarlette, A., Sepulchre, R., and Leonard, N.E. (2009). Autonomous rigid body attitude synchronization. *Automatica*, 45(2), 572–577.
- Schaub, H., Junkins, J.L., et al. (1996). Stereographic orientation parameters for attitude dynamics: A generalization of the rodrigues parameters. *Journal of the Astronautical Sciences*, 44(1), 1–19.
- Shahvali, M., Azarbahram, A., Naghibi-Sistani, M.B., and Askari, J. (2020). Bipartite consensus control for fractional-order nonlinear multi-agent systems: An output constraint approach. *Neurocomputing*, 397, 212–223.
- Shahvali, M., Pariz, N., and Akbariyan, M. (2018). Distributed finite-time control for arbitrary switched nonlinear multi-agent systems: an observer-based approach. *Nonlinear Dynamics*, 94(3), 2127–2142.
- Shuster, M.D. et al. (1993). A survey of attitude representations. *Navigation*, 8(9), 439–517.
- Tian, X., Liu, H., and Liu, H. (2018). Robust finite-time consensus control for multi-agent systems with disturbances and unknown velocities. *ISA transactions*, 80, 73–80.
- Tsiotras, P. (1996). Stabilization and optimality results for the attitude control problem. *Journal of guidance, control, and dynamics*, 19(4), 772–779.
- Wang, G., Wang, C., Li, L., and Zhang, Z. (2017). Designing distributed consensus protocols for second-order nonlinear multi-agents with unknown control directions under directed graphs. *Journal of the Franklin Institute*, 354(1), 571–592.
- Wang, Y. and Gao, Z. (2014). Consensus algorithms for second-order nonlinear multi-agent systems using backstepping control. In *Proceeding of the 11th World Congress on Intelligent Control and Automation*, 3505–3510. IEEE.
- Wu, Y., Zhang, H., Wang, Z., Zhang, C., and Huang, C. (2022). Leader-following and leaderless consensus of linear multiagent systems under directed graphs by double dynamic event-triggered mechanism. *IEEE Transactions on Systems, Man, and Cybernetics: Systems*.
- Zhao, L., Yu, J., and Lin, C. (2019). Distributed adaptive output consensus tracking of nonlinear multi-agent systems via state observer and command filtered backstepping. *Information Sciences*, 478, 355–374.
- Zhou, S., Liu, W., Wu, Q., and Yin, G. (2015). Leaderless consensus of linear multi-agent systems: matrix decomposition approach. In *2015 7th International Conference on Intelligent Human-Machine Systems and Cybernetics*, volume 2, 327–331. IEEE.